

## Metallic and insulating phases of $\text{Li}_x\text{C}_{60}$ , $\text{Na}_x\text{C}_{60}$ , and $\text{Rb}_x\text{C}_{60}$

C. Gu, F. Stepniak, D. M. Poirier, M. B. Jost, P. J. Benning, Y. Chen, T. R. Ohno, José Luís Martins, and J. H. Weaver

*Department of Materials Science and Chemical Engineering, University of Minnesota, Minneapolis, Minnesota 55455*

J. Fure and R. E. Smalley

*Rice Quantum Institute and Departments of Chemistry and Physics, Rice University, Houston, Texas 77251*

(Received 5 December 1991)

Photoemission studies of Li and Na fullerides show a band of alkali-metal-induced states that is fully below the Fermi level for a stoichiometry of  $\text{A}_2\text{C}_{60}$  and inverse photoemission results show a splitting of the unoccupied bands. Equivalent results for the Rb fullerides show the formation of only a metallic phase,  $\text{Rb}_3\text{C}_{60}$ . For all three fullerides, doping to saturation produces nonmetallic  $\text{A}_6\text{C}_{60}$  phases.

Recent studies showing superconductivity in certain alkali-metal-doped  $\text{C}_{60}$  fullerides<sup>1-6</sup> have led to experimental and theoretical efforts that have sought to correlate the electronic structure with superconductivity and other properties. It is now known that K and Rb fullerides form a superconducting fcc-based  $\text{A}_3\text{C}_{60}$  phase<sup>2,7</sup> and that solid solutions of K, Rb, and Cs give transition temperatures,  $T_c$ , that scale with the lattice constant.<sup>4,5</sup> Models have been proposed that associate  $T_c$  with the density of states at the Fermi level,  $E_F$ , reflecting narrowing of the band derived from the lowest unoccupied molecular orbitals (LUMO) of the fullerene with increasing  $\text{C}_{60}$ - $\text{C}_{60}$  distance.<sup>5</sup> Spectroscopic investigations have demonstrated partial filling of LUMO-derived bands for  $\text{K}_3\text{C}_{60}$ ,<sup>8-11</sup> and complete filling for  $\text{K}_6\text{C}_{60}$  where the latter is a new insulator with a bcc-derived structure and K ions in tetrahedral sites.<sup>12</sup> Superconductivity has been conspicuously absent in  $\text{Li}_x\text{C}_{60}$ ,  $\text{Na}_x\text{C}_{60}$ , and the  $\text{C}_{70}$ -based fullerides. While the Li and Na fullerides have resistivities 1-2 orders of magnitude higher than  $\text{K}_x\text{C}_{60}$ ,<sup>13</sup> the distribution and population of the electronic states for these fullerides have not been determined. Such investigations are critical if models of the normal state are to be developed for the full family of fullerides and superconductivity is to be understood.

This paper focuses on the electronic states of the Li, Na, and Rb fullerides. Photoemission and inverse photoemission results demonstrate that Na mixing produces only semiconducting molecular solids, including phases that are probably  $\text{Na}_2\text{C}_{60}$  and  $\text{Na}_6\text{C}_{60}$ . Results for  $\text{Li}_x\text{C}_{60}$  reveal equivalent spectral changes. In contrast, a metallic band forms for  $\text{Rb}_3\text{C}_{60}$  and there is a distinct Fermi-level cutoff, as for  $\text{K}_3\text{C}_{60}$ .<sup>8-11</sup> Our results suggest that for all alkali-metal- $\text{C}_{60}$  mixtures the valence electron of the alkali-metal atom is transferred to the threefold-degenerate LUMO-derived states of  $\text{C}_{60}$ . This charge transfer is consistent with theoretical local-density calculations. The observation of semiconducting phases with compositions between  $\text{C}_{60}$  and  $\text{A}_6\text{C}_{60}$  requires either a crystal-field splitting of the  $t_{1u}$  LUMO-derived states, or a metal-insulator transition driven by electron correlation effects.

The procedures for preparation of high-purity  $\text{C}_{60}$  have

been described elsewhere.<sup>14</sup> For our studies, thin films of  $\text{C}_{60}$  were formed and then doped with alkali metals using conventional ultrahigh vacuum vapor deposition techniques.<sup>8,11</sup> Prior to film formation, the  $\text{C}_{60}$  and the alkali-metal SAES getter sources were degassed so that film growth could be done at pressures of  $2 \times 10^{-10}$  Torr or better. A Pt foil was used as a substrate for the  $\text{Li}_x\text{C}_{60}$  and  $\text{Rb}_x\text{C}_{60}$  studies, as well as for  $\text{Na}_x\text{C}_{60}$ . The Pt foil was cleaned by repeated annealing to  $1100^\circ\text{C}$ , and the sharp Fermi-level cutoff of Pt served both as an energy reference and a measure of the experimental resolution. Cleaved surfaces of GaAs(110) were used for the  $\text{Na}_x\text{C}_{60}$  photoemission and inverse photoemission studies. The  $\text{C}_{60}$  films were  $\sim 100$  Å thick, as monitored with a quartz oscillator. Spectra for pristine  $\text{C}_{60}$  showed valence- and conduction-band features that were identical to those discussed previously.<sup>15-17</sup> Alkali-metal incorporation involved exposure to the source for predetermined amounts of time. Spectroscopic studies were done following growth at 300 K and after annealing to enhance crystal growth and intermixing. The stoichiometries were determined from the relative emission intensity of the LUMO-derived band for both photoemission and inverse photoemission. Strictly speaking, this determines the average number of electrons transferred to a  $\text{C}_{60}$  molecule, which is equal to the number of ions in the case of formal charge transfer. Saturation exposure produced a filled LUMO-derived band, taken to be  $\text{A}_6\text{C}_{60}$ . In the photoemission work, an independent determination of stoichiometry could be made using the Li  $1s$ , Na  $2p$ , or Rb  $3d$  core-level emission intensities, similar to the study on  $\text{K}_x\text{C}_{60}$ .<sup>11</sup> We estimate an uncertainty in  $x$  of  $\pm 0.5$  for the inverse photoemission measurements and  $\pm 0.3$  for the photoemission measurements, with higher confidence levels near  $x=0$  and 6.

Figure 1 shows valence-band spectra referenced to the Fermi level of the spectrometer for  $\text{Li}_x\text{C}_{60}$ . The spectra were acquired with  $h\nu=65$  eV, and additional results were obtained with  $h\nu=50$  eV. The spectral features reflect the distribution of levels in the ground state shifted in energy by screening of the hole created by the removal of an electron.<sup>18</sup> The two  $p_\pi$ -derived  $\text{C}_{60}$  features within 5 eV of  $E_F$  have fivefold and ninefold degeneracy.<sup>15</sup> The fact that they have opposite symmetries influences their

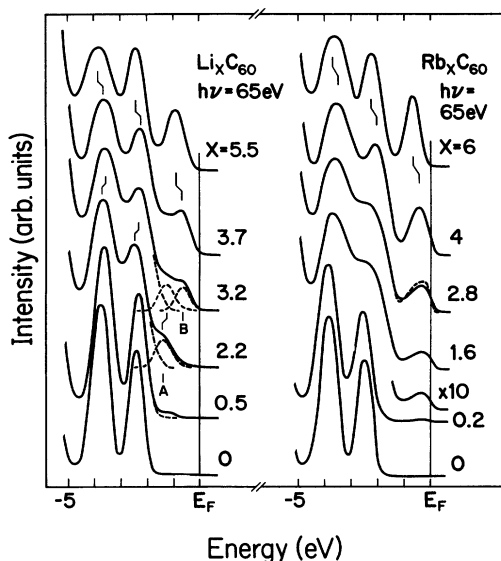


FIG. 1. Photoemission spectra for  $\text{Li}_x\text{C}_{60}$  and  $\text{Rb}_x\text{C}_{60}$  with energies referenced to the Fermi level of the spectrometer,  $E_F$ . The nonmetallic behavior of  $\text{Li}_x\text{C}_{60}$  for all  $x$  values is indicated by the lack of emission at  $E_F$ . In contrast,  $\text{Rb}_x\text{C}_{60}$  films exhibit metallic Fermi edges. Doping to  $\text{A}_6\text{C}_{60}$  produces complete filling of the LUMO-derived band and recovery to the insulating molecular-solid configuration. The dashed lines for  $\text{Li}_x\text{C}_{60}$  provide a guide to the eye for bands *A* and *B*. That for  $\text{Rb}_{2.8}\text{C}_{60}$  shows the effect of enhanced experimental resolution.

relative intensities.<sup>19</sup>

Li deposition to produce  $\text{Li}_{0.5}\text{C}_{60}$  yields a photoemission peak, labeled *A*, that is centered 1.1 eV above the center of the band derived from the highest occupied molecular orbitals (HOMO) (full width at half maximum, FWHM,  $\sim 0.8$  eV). This HOMO-to-*A* separation is smaller than any estimate of the separation between centers of the HOMO and LUMO bands or the band gap of fcc  $\text{C}_{60}$ .<sup>20</sup> The intensity of peak *A* increased with Li exposure until  $x \cong 2$ , as depicted in Fig. 1 by the dashed line that serves as a guide to the eye. Another feature appeared with continued Li incorporation, centered 0.6 eV closer to  $E_F$  (FWHM 0.7 eV), and this feature, labeled *B*, grew at the expense of feature *A*.  $E_F$  was pinned at the top of peak *B* when it appeared, presumably because of holes in the evolving phase characterized by peak *B*, and the valence-band structures shifted accordingly. When saturation was reached,  $x = 6$ , the spectral features sharpened and shifted away from  $E_F$ . This is consistent with improved sample homogeneity, the filling of the LUMO levels, the loss of defects that pin  $E_F$  near the top of peak *B*, and the molecular character of  $\text{A}_6\text{C}_{60}$  solids.<sup>8,11</sup> Throughout Li- $\text{C}_{60}$  mixing, the density of states at  $E_F$  was minimal. Peak *B* was centered 1.5 eV above HOMO, as is evident for  $\text{Li}_6\text{C}_{60}$ . A comparison shows a striking similarity between the saturated phase and  $\text{K}_6\text{C}_{60}$ ,<sup>8-11</sup> a bcc-based structure.<sup>12</sup>

Analysis of the Li  $1s$  core-level line shape shows a single main line 55.2 eV below HOMO for  $x \lesssim 2$  (1 eV FWHM). For  $x \gtrsim 2$ , a second feature appeared shifted 1.2 eV to higher binding energy. This reflects an energy-

loss process in which electrons propagating through the lattice scatter inelastically and induce transitions from band *B* to the lowest empty molecular state of  $\text{Li}_6\text{C}_{60}$ . The analogous  $\pi$ - $\pi^*$  dipole excitation has been observed as a satellite of the C  $1s$  emission for  $\text{K}_6\text{C}_{60}$ .<sup>21</sup> Its presence serves as another indicator of phase separation during Li incorporation. Similar energy-loss satellites appear in the Na  $2p$  and Rb  $3d$  lines for  $\text{Na}_6\text{C}_{60}$  (at 1.0 eV) and  $\text{Rb}_6\text{C}_{60}$  (at 1.1 eV).

Li has the highest melting point (454 K), the highest cohesive energy (1.63 eV/atom), and the highest ionization potential (5.39 eV) of the alkali metals, and we were concerned that Li clusters might form on the  $\text{C}_{60}$  film. To demonstrate facile mixing of Li and  $\text{C}_{60}$ , we deposited a thick layer of Li on Pt and condensed successive amounts of  $\text{C}_{60}$ , in increments of 30 Å. Photoemission spectra for the composite following annealing at 100 °C were very similar to those discussed below but in reverse order because the saturated phase appeared first and the low- $x$  phase was reached only when the Li source was depleted or diffusion was kinetically limited.

The right panel of Fig. 1 summarizes photoemission results for  $\text{Rb}_x\text{C}_{60}$ . Comparison to those for  $\text{Li}_x\text{C}_{60}$  reveals fundamental differences in the occupation of the LUMO-derived band. In particular, a distinct Fermi edge was evident for  $x = 0.2$ , and the LUMO-derived valence feature grew monotonically with  $x$ , with no change in binding energy or general line shape until after  $x = 3$ . This is consistent with phase separation into  $\text{Rb}_3\text{C}_{60}$  and  $\alpha$ - $\text{C}_{60}$ .<sup>22</sup> The instrumental resolution for the solid curves in Fig. 1 was 0.34 eV and that for the dashed curve for  $x = 2.8$  was 0.16 eV. The width of the Fermi edge was equal to that expected when account is taken of thermal broadening at 300 K.

The photoemission results for  $\text{Rb}_x\text{C}_{60}$  are very similar to those discussed in detail for  $\text{K}_x\text{C}_{60}$ .<sup>8-11</sup> The 10 K increase in  $T_c$  (Refs. 1-3) can be explained by a  $\sim 10\%$  increase in the density of states at  $E_F$  in a model where superconductivity is due to the coupling of electrons to the molecular vibrations of  $\text{C}_{60}$ .<sup>5,8,23</sup> Such an effect should accompany the expansion of the fcc lattice induced by incorporation of the larger Rb ion and the narrowing of the LUMO-derived band (Rb ionic radius 1.48 Å vs 1.33 Å for K). It is not possible to quantitatively identify a small increase in the emission intensity at  $E_F$ , particularly given the dependence on phonon scattering and photohole lifetimes. We also note that the LUMO band is much wider and all other spectral features are broadened in metallic  $\text{Rb}_3\text{C}_{60}$  with respect to insulating  $\text{C}_{60}$  or insulating  $\text{Rb}_6\text{C}_{60}$ . Local-density calculations for  $\text{C}_{60}$  and  $\text{K}_3\text{C}_{60}$  show minimal changes in the width of the LUMO-derived band.<sup>23,24</sup>

The results of Fig. 1 show that emission from the Li- and Rb-induced bands develops in fundamentally different ways. Those differences raise questions about the conversion of empty states into occupied states during compound formation. Such issues can be examined by combining photoemission and inverse photoemission, as summarized in Fig. 2 for  $\text{Na}_x\text{C}_{60}$ . In this case,  $\text{Na}_x\text{C}_{60}$  films were prepared on Pt or cleaved GaAs(110) and the samples were annealed at  $\sim 100$  °C for 10 min after each

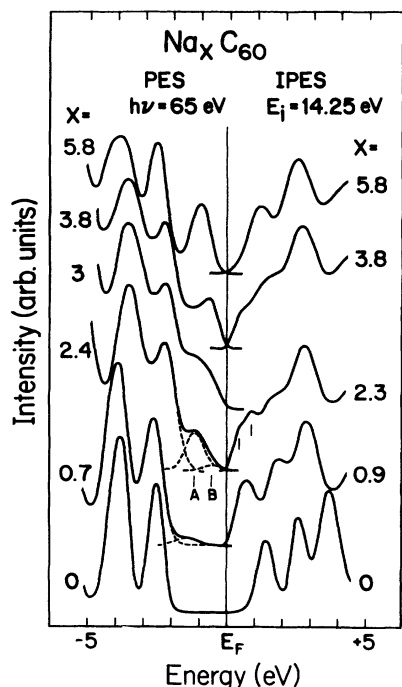


FIG. 2. Photoemission and inverse photoemission results for  $\text{Na}_x\text{C}_{60}$ , showing the evolution of the occupied and empty states near  $E_F$ . Feature *A* corresponds to  $\text{Na}_2\text{C}_{60}$  and feature *B* reflects conversion to the  $\text{Na}_6\text{C}_{60}$  phase. For  $\text{Na}_{2.3}\text{C}_{60}$ , splitting is evident in the leading conduction-band feature. The movement of spectral features relative to  $E_F$  reflects changes in screening with pinning of  $E_F$  at the conduction-band minimum.

deposition. The photoemission results reveal the formation of band *A* well below  $E_F$  for  $x \lesssim 2$  and the formation of band *B*, shifted 0.6 eV for  $x \gtrsim 2$ . The striking similarity to  $\text{Li}_x\text{C}_{60}$  suggests that the overall properties are the same for the two fullerides.

Inverse photoemission spectra (IPES) for  $\text{Na}_x\text{C}_{60}$  were acquired with an incident electron energy,  $E_i$ , of 14.25 eV under conditions that gave  $\sim 0.3$  eV resolution. The first two features of the empty states for pure  $\text{C}_{60}$  have threefold degeneracy and are predominantly  $\pi$  derived.<sup>16,17</sup> The third empty state feature has contributions from both  $\pi$  and nonmolecular-type states, indicating the presence of intermolecular interactions.<sup>16,17</sup> The incorporation of small amounts of Na produces a rigid shift of the empty state features toward  $E_F$ , with Fermi-level pinning at the edge of the conduction-band minimum (CBM). With increased Na incorporation, the empty state features broaden and there is reduced emission from the LUMO-derived band. Two distinct peaks separated by  $\sim 0.5$  eV can be resolved near the CBM for  $x \cong 2$ . This splitting may reflect the formation of a pair of singly degenerate bands as a result of reduced symmetry in the  $x = 2$  phase, with feature *A* in the valence bands reflecting the third LUMO-derived band. (This structure could also reflect the superposition of LUMO features related to  $x = 2$  and 4 phases,<sup>24</sup> but the occupied-state features give no clear indication of an  $x = 4$  phase.) The emission from these bands diminishes and ultimately is very small, as shown for  $x = 5.8$ . In the Na-saturated phase, the lowest

conduction-band structure is derived from states that were originally the LUMO+1 levels, and its separation from the next empty state is greater than for pure  $\text{C}_{60}$  (1.4 eV vs 1.0 eV). We attribute the dilation to band-structure effects in the bcc fulleride. We also note that Na exposure at 300 K without annealing produced a saturated state where the spectral features suggest Fermi-level pinning near the CBM. Annealing to 100 °C produced a slightly alkali-metal-deficient  $\text{Na}_6\text{C}_{60}$  phase because Na was desorbed, an effect observed for the occupied states as well.

These results for the Li, Na, and Rb fullerides, together with those for the K fullerides,<sup>8–11</sup> demonstrate very clear differences in the distribution of electronic states. For  $\text{K}_3\text{C}_{60}$ , the occupation of the LUMO-derived bands is understood in terms of complete charge transfer from K to the LUMO level for a structure having ions in the tetrahedral and octahedral sites of the fcc lattice. LDA calculations have demonstrated minimal perturbation of the wave functions of the fullerite by the K ions,<sup>23</sup> and analogous results are expected for  $\text{Rb}_3\text{C}_{60}$ . Complete filling of the LUMO-derived band for  $x = 6$  occurs for all four fullerides, most likely because the alkali-metal ions occupy all of the possible tetrahedral interstices of the bcc structure. In contrast, the  $\text{Li}_2\text{C}_{60}$  and  $\text{Na}_2\text{C}_{60}$  results show a single band well below  $E_F$  and splitting of the empty states. Based on the structural data for the other alkali-metal fullerides,<sup>12,24</sup>  $\text{Li}_2\text{C}_{60}$  could form with Li ions in tetrahedral sites of the fcc lattice (antifluorite structure). This would be different from the  $\text{A}_3\text{C}_{60}$  structure since the octahedral sites would be empty, presumably because the  $\text{Li}^+$  ion is too small to stabilize the  $\text{Li}_3\text{C}_{60}$  structure (octahedral radius 2.06 Å compared to ionic sizes of 0.68 Å for Li and 0.97 Å for Na). Another structural possibility would be a bcc-derived structure similar to the observed  $\text{A}_4\text{C}_{60}$  phases<sup>25</sup> with partial tetrahedral site occupancy.

The observation of  $\text{Li}_2\text{C}_{60}$  and  $\text{Na}_2\text{C}_{60}$  semiconducting phases raises the question of whether they are band insulators or whether their insulating character is due to electron correlation effects. The spectra of Fig. 2 are consistent with the transfer of the valence electron of the alkali-metal atoms to the threefold-degenerate LUMO-derived states of  $\text{C}_{60}$ . Local-density calculations also find charge transfer.<sup>23</sup> The calculated band structures of  $\text{C}_{60}$  and  $\text{K}_3\text{C}_{60}$  show only a rigid shift of the LUMO-derived states with alloying,<sup>23</sup> so that a large crystal-field splitting of those levels in  $\text{Li}_2\text{C}_{60}$  and  $\text{Na}_2\text{C}_{60}$  appears unlikely. In particular, if the Li and Na atoms occupy the small tetrahedral interstitials of an fcc crystal, such splitting is ruled out by group-theory arguments. On the other hand, there are several indications that the alkali-metal fullerides have strongly correlated electrons and could be close to the metal-insulator transition. First, the measured conductivities of the alkali-metal fullerides<sup>13</sup> are quite low and the mean free paths derived from those values are a few angstroms. Reflectivity measurements of  $\text{Rb}_3\text{C}_{60}$  suggest a mean free path of 10–20 Å.<sup>26</sup> Mean free paths close to the  $\text{C}_{60}$ - $\text{C}_{60}$  intermolecular distance are an indication that we are close to a metal-insulator transition.<sup>27</sup> Another measure of the importance of correlation

effects is the magnitude of the electron-electron interaction parameter  $U$ . For gas phase  $\text{C}_{60}^-$ , the energy difference between the center of the HOMO- and LUMO-derived bands is  $\sim 2.0$  eV.<sup>28</sup> This energy is 1.5 eV in the saturated  $\text{A}_6\text{C}_{60}$  fullerenes where the LUMO-derived band is filled. For the  $\text{C}_{60}$  fullerite, the lowest excitation energy is believed to be approximately 1.9 eV.<sup>15</sup> However, the combination of photoemission and inverse photoemission gives a center-to-center separation of  $\sim 3.8$  eV for the HOMO and LUMO bands, and the difference is a measure of the electron-electron interaction parameter  $U$  in solid  $\text{C}_{60}$ , giving  $U \sim 2.0$  eV. From Fig. 2, the separation between feature  $A$  (photoemission) and the lowest conduction-band feature (inverse photoemission) for  $\text{Na}_2\text{C}_{60}$  is  $\sim 1.6$  eV. This is close to  $U$  in magnitude and is therefore consistent with a band split by correlation

effects.

We also note that the occupied band width of  $\text{Rb}_3\text{C}_{60}$  (Fig. 1) and  $\text{K}_3\text{C}_{60}$  (Refs. 8 and 10) is  $\sim 1$  eV, which is larger than the calculated total bandwidth of  $\sim 0.5$  or the observed width of the peaks of the LUMO-derived states (Figs. 1 and 2) in the insulating phases. This is hard to reconcile with a rigid band picture and may be another sign of the importance of electron correlation in these materials.

This work was supported by the Office of Naval Research, the National Science Foundation, and the Robert A. Welch Foundation. The photoemission experiments were conducted at the Wisconsin Synchrotron Radiation Center, a facility supported by the National Science Foundation.

- <sup>1</sup>A. F. Hebard *et al.*, *Nature (London)* **350**, 600 (1991).  
<sup>2</sup>K. Holczer, O. Klein, S.-M. Huang, R. B. Kaner, K.-J. Fu, R. L. Whetten, and F. Diederich, *Science* **252**, 1154 (1991).  
<sup>3</sup>M. J. Rosseinsky *et al.*, *Phys. Rev. Lett.* **66**, 2830 (1991).  
<sup>4</sup>C.-C. Chen, S. P. Kelty, and C. M. Lieber, *Science* **253**, 886 (1991); S. P. Kelty, C.-C. Chen, and C. M. Lieber, *Nature (London)* **352**, 223 (1991).  
<sup>5</sup>R. M. Fleming, A. P. Ramirez, M. J. Rosseinsky, D. W. Murphy, R. C. Haddon, S. M. Zahurak, and A. V. Makhija, *Nature (London)* **352**, 787 (1991).  
<sup>6</sup>K. Tanigaki, T. W. Ebbesen, S. Saito, J. Mizuki, J. S. Tsai, Y. Kubo, and S. Kuroshima, *Nature (London)* **352**, 222 (1991).  
<sup>7</sup>P. W. Stephens, L. Mihaly, P. L. Lee, R. L. Whetten, S.-M. Huang, R. Kaner, F. Diederich, and K. Holczer, *Nature (London)* **351**, 632 (1991).  
<sup>8</sup>P. J. Benning, J. L. Martins, J. H. Weaver, L. P. F. Chibante, and R. E. Smalley, *Science* **252**, 1417 (1991).  
<sup>9</sup>G. K. Wertheim, J. E. Rowe, D. N. E. Buchanan, E. E. Chaban, A. F. Hebard, A. R. Kortan, A. V. Makhija, and R. C. Haddon, *Science* **252**, 1419 (1991).  
<sup>10</sup>C. T. Chen *et al.*, *Nature (London)* **352**, 603 (1991).  
<sup>11</sup>P. J. Benning, D. M. Poirier, T. R. Ohno, Y. Chen, M. B. Jost, F. Stepniak, G. H. Kroll, J. H. Weaver, J. Fure, and R. E. Smalley, *Phys. Rev. B* (to be published).  
<sup>12</sup>O. Zhou *et al.*, *Nature (London)* **351**, 462 (1991).  
<sup>13</sup>R. C. Haddon *et al.*, *Nature (London)* **350**, 320 (1991).  
<sup>14</sup>R. E. Haufler *et al.*, *J. Phys. Chem.* **94**, 8634 (1990).  
<sup>15</sup>J. H. Weaver *et al.*, *Phys. Rev. Lett.* **66**, 1741 (1991).  
<sup>16</sup>M. B. Jost, N. Troullier, D. M. Poirier, J. H. Weaver, L. P. F. Chibante, and R. E. Smalley, *Phys. Rev. B* **44**, 1966 (1991).  
<sup>17</sup>J. L. Martins, N. Troullier, and J. H. Weaver, *Chem. Phys. Lett.* **180**, 457 (1991).  
<sup>18</sup>T. R. Ohno, Y. Chen, S. E. Harvey, G. H. Kroll, J. H. Weaver, R. E. Haufler, and R. E. Smalley, *Phys. Rev. B* **44**, 13747 (1991).  
<sup>19</sup>P. J. Benning, D. M. Poirier, N. Troullier, J. L. Martins, J. H. Weaver, R. E. Haufler, L. P. F. Chibante, and R. E. Smalley, *Phys. Rev. B* **44**, 1962 (1991).  
<sup>20</sup>N. Troullier and J. L. Martins (unpublished).  
<sup>21</sup>D. M. Poirier, T. R. Ohno, G. H. Kroll, Y. Chen, P. J. Benning, J. H. Weaver, L. P. F. Chibante, and R. E. Smalley, *Science* **253**, 646 (1991).  
<sup>22</sup>Q. Zhu, O. Zhou, N. Coustel, G. Vaughan, J. P. McCarley, Jr., W. J. Romanow, J. E. Fischer, and A. B. Smith III, *Science* **254**, 545 (1991).  
<sup>23</sup>J. L. Martins and N. Troullier (unpublished); M. Schluter, M. Lannoo, M. Needels, G. A. Baroff, and D. Tomanek, *Phys. Rev. Lett.* **68**, 526 (1992).  
<sup>24</sup>M.-Z. Huang, Y.-N. Xu, and W. Y. Ching (unpublished).  
<sup>25</sup>R. M. Fleming *et al.*, *Nature (London)* **352**, 702 (1991).  
<sup>26</sup>L. D. Rotter *et al.*, *Nature (London)* (unpublished).  
<sup>27</sup>N. F. Mott, *Metal-Insulator Transitions* (Taylor & Francis, London, 1990).  
<sup>28</sup>R. E. Haufler, L.-S. Wang, L. P. F. Chibante, C. Jin, J. J. Conceicao, Y. Chai, and R. E. Smalley, *Chem. Phys. Lett.* **182**, 491 (1991).